Simulation of a Micro Optical Distance Sensor Realized by the LIGA Process

H. Guth*, A. Hellmann*, I. Sieber*, H. Eggert*, J. Mohr**,
H. Nakajima***, K. Tanimot*** T. Usami***

*Institut für Angewandte Informatik, **Institut für Mikrostrukturtechnik
Forschungszentrum Karlsruhe GmbH, P.O.Box 3640, D-76021 Karlsruhe, Germany, guth@iai.fzk.de
***Sensing System Dept. Industrial Electronics & Systems Lab., Mitsubishi Electric Corp.,
Tsukaguchi-Honmachi 8-1-1, Amagasaki, Hyogo, 661-8661 Japan, haijime@con.sdl.melco.co.jp

ABSTRACT

The aim of the presented work is to simulate and validate an ultra miniaturized optical distance sensor, which works by means of triangulation. The sensor is dedicated for a detection range of 1 to 6mm and has been designed by Mitsubishi Electric Corporation and realized in cooperated research with the Forschungszentrum Karlsruhe (FZK) [1].

In a first step the structure of a monolithic manufactured device is shown. Then the composition of the simulation model is described and presented by means of raytracing. Simulation results are given as analyzed irradiation distributions of the target spots. Further simulation results concern irradiation distribution analyses at the location of the corresponding detection devices. As far as experimental results are available they are compared to the simulated ones.

Keywords: free-space optics, microoptical simulation, microoptical sensor, LIGA technology, distance sensor.

INTRODUCTION

The LIGA process (characterized by the three steps: deep-X-ray lithography, electroforming, plastic molding) has been developed at the FZK and is used to manufacture microoptical systems. This process allows micro components of arbitrary two dimensional geometry and structural height of several hundred micrometers to be produced to high accuracy [2]. This technique can be used not only to manufacture individual optical components like cylindrical lenses, but also to produce mountings on a substrate, which are used to arrange the individual components as with microoptical benches. Even complete microoptical devices with elements adjusted to each other can be fabricated, for example the microoptical distance sensor, which is described in the following.

The base of the microoptical sensor is a planar waveguide, composed of three welded layers of resist film bonded on a ceramic substrate. The material of the core layer is polymethylmethacrylate (PMMA) with a refractive index of 1.491 and the cladding material is a copolymer with a refractive index of 1.4725 [1]. This three layer waveguide is processed by deep X-ray lithography, the first step of the LIGA process, to obtain the lateral structure [3], described in figure 1. The side walls of the waveguide, produced in this manner, act as both mirrors for deflecting the light in the lateral direction and as alignment structures for optical components like fibers and lenses. In this way a monolithic system is realized which works by means of triangulation.

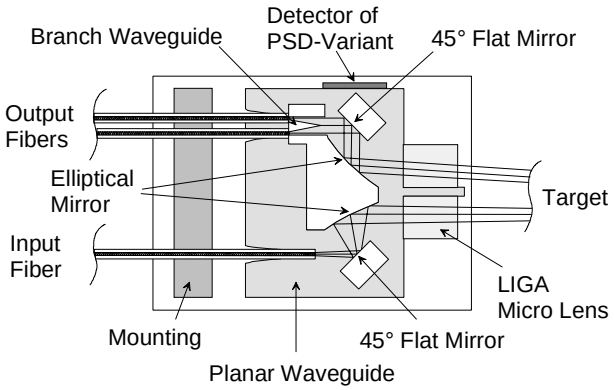

Figure 1: Top view of the sensor design. The optical path of the first design variant is shown. The second variant is produced by removing the 45° flat mirror of the detection part and placing a position sensitive detector (PSD) at the side wall of the waveguide.

SENSOR DESIGN

Optical systems for distance measurement based on triangulation are composed of two parts. The first, which produces a spot on the target whose distance is to be measured and the second, which images this spot on a detecting device. The first part, producing the spot, consists of an input fiber, connected to the planar waveguide and flat and elliptical mirrors, embedded in the guide for deflecting and collimating the beam in the lateral direction. The function of the horizontal cylindrical lens is to collimate the beam in the perpendicular direction. The imaging part of the system consists of the same cylindrical lens as in the first part for focussing the diffused light from the spot at the target to the guiding layer of the subsequent

planar waveguide. The elliptical and flat mirrors, embedded in the guide, focus and deflect the light on the detection device as shown in figure 1.

There exist two different design variants of the detection device. One of them is using two output fibers whereas the intensity ratio of them is a direct measure of the distance. The incoupling of the beam into the output fibers is done by a special beamsplitter using a sharp edge as dividing point. This variant has the advantage not to have electrical components locally at the sensor. The other variant has no flat mirror and directly focuses the beam from the elliptical mirror onto a position sensitive detector (PSD) assembled at the side wall of the planar waveguide. In this case the center of gravity of the irradiance distribution is the measure for the corresponding distance.

The parameters of the elliptical mirror of the probe part are chosen such that one focus point of the ellipse is at the interface position of the incoupling fiber and the other focus point is at the mean position of the measurement range of the distance sensor. The elliptical mirror of the detection part is designed in this way that the irradiated target spot at this mean position is imaged at the dividing point of the beamsplitter or at a special point of the PSD, respectively. Further design variants of the elliptical mirrors are provided for other measurement ranges.

There also exist different design variants of the cylindrical lens which focuses the rays in the perpendicular direction.

SENSOR SIMULATION MODEL

As the optical design software package SOLSTIS™* is used to simulate the optical property of the distance sensor, the conventions concerning this software system are taken into account.

The system is modeled neglecting the flat mirrors because they do not effect the imaging. A graded index fiber of 50µm core and a numerical aperture of 0.2 is defined as light source.

The planar three layer waveguide is built using the non-sequential propagation component MULTIGUIDE which allows rectangular multi-layer structures by stacking surfaces and giving a refractive index for each layer. The special lateral structure of the waveguide is taken into account by composing consecutive multiguide components each with a core layer of 50µm and refractive index of 1.491 (refractive index of cladding layers: 1.4725). Special care is to be taken to choose the lateral dimensions so that no reflection at side walls is possible.

The elliptical mirrors, embedded in the waveguide, are realized as surfaces between consecutive waveguide elements. The perpendicular (with respect to the planar waveguide) side walls forming the mirrors are obtained by applying a cylinder function to the surface. Two spherical surfaces, each with a cylinder function and individual refractive index yield the cylindrical lens at the end of the probe part waveguide and in front of the detection part waveguide, respectively.

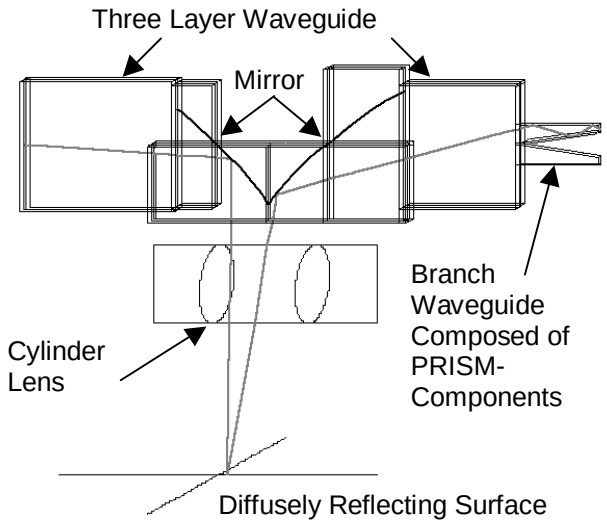

Figure 2: Three dimensional representation of the simulation model. An inclined ray from the input fiber through the probe part of the device (left half) to the produced spot at the diffusely reflecting target surface is shown. As a representative a ray of this spot is propagated through the detection part (right half) and the branch waveguide into the upper output fiber. In the PSD case a screen is installed at that position instead of the branch waveguide.

The branch waveguide, acting as beamsplitter for coupling the rays into the output fibers is modeled using the non-sequential propagation component PRISM. This component allows to create a complex three dimensional structure by defining a number of flat surfaces with individual characteristics, which form the boundary of the structure. The step index output fibers, each with a core diameter of 110µm, are simulated by the photometry element RECEIVER, which considers the numerical aperture of the output fibers. In the PSD case instead of the branch guide a simple image is used, which shows the irradiation distribution at positions according to the measurement distances. The diffusely reflecting target, the distance of which is to be measured, is represented by a reflecting surface with the DIFFUSION function, which allows to take into account arbitrary combinations of Lambertian and Gaussian scattering.

Figure 2 represents a three dimensional ray-tracing plot, which schematically shows both, the optical components and the propagation of a slightly inclined beam through the device.

SIMULATION CALCULATIONS

The photometric simulation of the system is carried out step by step, using the SOLSTIS™ system for calculating

*OPTIS, BP275, France-83078 Toulon cedex 9

irradiance distributions. These calculations provide two dimensional intensity maps. Corresponding experimental maps of a prototype device are recorded using a CCD camera. All maps are analyzed by the momentum calculation procedure proposed by ISO [4]. In a first step the probe beam, producing the spot at the "distant" target, is investigated. Then the detection part of the sensor is simulated.

Target Spot

The probe beam is quantified and the irradiation distribution of the spot at the target position is calculated using 10,000,000 rays, which are propagated from the input fiber through the planar waveguide of the probe part. Comparing the simulated and the experimentally recorded spots it can be seen, that the shapes are different at different target distances but the shapes of the simulated and corresponding measured distributions are very similar. However comparing the parameters of the calculated and corresponding measured spots the simulated distributions show smaller beam width than the measured ones, as represented in figure 3.

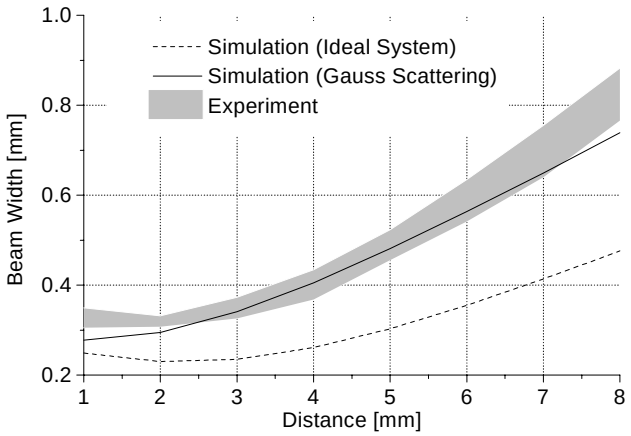

Figure 3: Lateral beam width at the target position depending on the target distance. The parameters of the experimentally recorded target maps are calculated using different background correction methods and produce values represented by the gray area. The simulation of the ideal system resulted in lateral width represented by the dashed line. Applying Gaussian scattering to some surfaces, the width values change to those represented by the solid line.

This fact leads to the assumption that diffusion has to be assigned to the reflecting and output surfaces of the LIGA-produced waveguide walls. Investigations showed that applying a Gaussian diffusion at a rate of 100% with a total angle of scattering distribution of 1.2° yields best results. In the following all further side walls of the planar waveguide which refract or reflect the rays are treated by this diffusion function for better approaching the reality.

Fiber Output

The second half of the distance sensor is the detection part, whereas two design variants exist. The first one has a branch waveguide with two output fibers which collect the distance dependent intensity distributions as shown in figure 4.

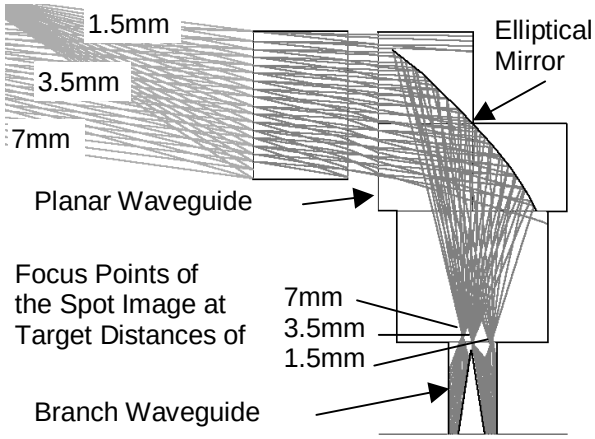

Figure 4: Ray-trace representation of the detection part of figure 2 (rotated clockwise by 90°). The drawn rays come from positions of three consecutively target distances. As one can see, the rays coming from the 3.5mm distant target position are focused at the dividing point position of the branch waveguide, whereas the other are collected only in the left or the right branch, respectively.

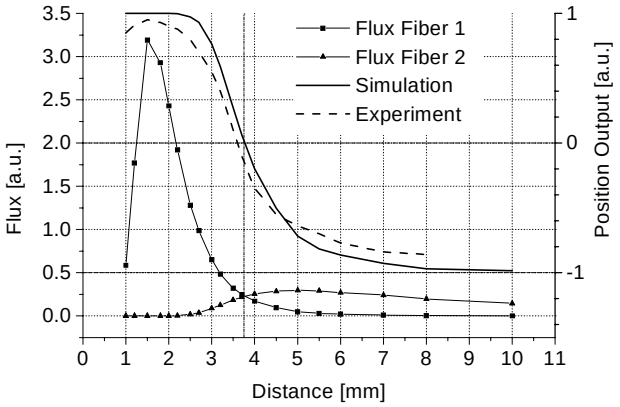

Figure 5: Graph of the fluxes of the two output fibers. The deduced position output ([fiber1-fiber2]/[fiber1+fiber2]) is also shown. The solid lines represent simulated results whereas the dashed line is calculated from the corresponding experiment.

The ray-tracing plot of figure 4 also reveals the reason for the diminished flux calculated in the branch of output fiber1 for very small target distances, as shown in figure 5. It can be seen, that even at the distance of 1.5mm some rays miss the lower part of the elliptical mirror and therefor cannot be reflected to the detector. If the distance is reduced further, this effect is increased.

As it is shown in figure 5, the agreement of the deduced "position output" of the simulation and of the experimental result, received from a prototype device is very similar. The small shift of the zero crossing position might be caused by asymmetrical irradiation distributions or by unbalanced photodiodes which measure the intensities of the light guided by the output fibers.

The lateral beam position at the entrance of the branch waveguide and the corresponding beam width, dependent on the target distance, is represented in figure 6. One can see the effect of broadening the beam width by considering diffusive Gaussian scattering at planar waveguide walls. It is also illustrated at which distances the beam misses or hits one or both of the branch entrances.

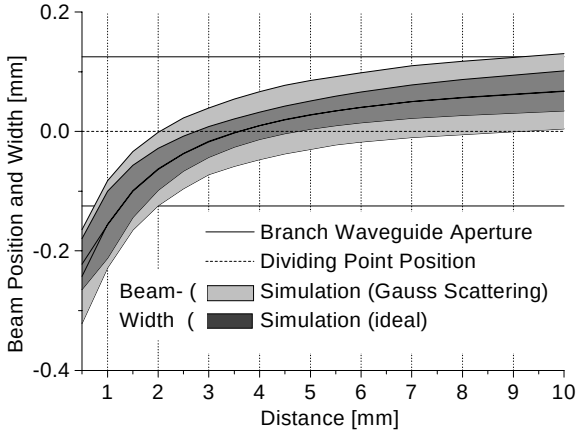

Figure 6: Diagram of the lateral beam position and width at the branch waveguide entrance of the ideal system and the system with Gaussian diffusion applied. Horizontal lines mark special positions – dashed line at 0.0mm: dividing point, solid lines at -/+0.125mm: entrance aperture of branch1 and branch2, respectively.

Position Sensitive Detector

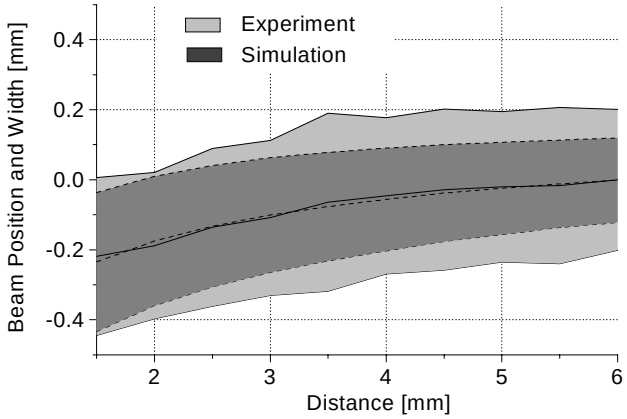

Figure 7: Representation of the lateral beam position and width of the PSD-variant of the detection part. The experimental data result from a CCD recording.

The second design variant of the detection part is obtained by omitting the branch waveguide with the output fibers and the flat mirror of the upper half of figure 1. So the image of the target spot is focused directly onto a position sensitive detector (PSD) at the side wall of the planar waveguide. To analyze this imaged spot, the PSD is left out and a CCD camera is used to record the irradiance distribution.

The diagram of figure 7 represents the distribution parameters of the experimentally recorded spot dependent on the target distribution. Caused by experimental set-up, the CCD camera could not be adjusted exactly. As a consequence the lateral beam width, shown in figure 7, is enlarged. Simulation calculations result in a dislocation of the camera of about 540µm. Nevertheless, the center of gravity of both, the experimental and the simulated results, is in a very good agreement.

CONCLUSION

Several variants of a microoptical distance sensor have been modeled and the optical properties have been simulated. The simulation results have been compared with corresponding experimental investigations, which revealed a good agreement. This led to the statement, that complex optical devices, to be produced by the LIGA technology, can be modeled and simulated, in order to lower the cost by reducing the number of test structures to be manufactured.

ACKNOWLEDGEMENT

The authors would like to thank Dr. Patrick Ruther and Mr. Stefan Senger for providing experimental measurements.

REFERENCES

[1] H. Nakajima, P. Ruther, J. Mohr, T. Nakashima, K. Takashima, T. Usami, "Micro optical distance sensor fabricated by the LIGA process", Proc. SPIE, Vol. 3513, 106-112, 1998.

[2] E.W. Becker W. Ehrfeld, P. Hagmann, A. Maner, D. Münchmeyer, "Fabrication of microstructures with high aspect ratios and great structural heights by syncrotron radiation, lithography, galvanoforming and plastic molding (LIGA process)", Microelectron. Eng., 4, 35-56, 1986.

[3] J. Mohr, B. Anderer, W. Ehrfeld, "Fabrication of a planar grating spectrograph by deep-etch lithography with synchrotron radiation", Sensors and Actuators A, 25-27, 571-575, 1991.

[4] International Organisation for Standardization, "Optics and optical instruments, Lasers and laser related equipment, Test methods for laser beam parameters: Beam width, divergence angle and beam propagation factor", Provis. Manuscript for ISO/DIS 11146, ISO/TC 172/SC 9/WG1 N73, DIN Germany, 1994.